# Effects of Desiccation on the Hydraulic Conductivity Versus Void Ratio Relationship for a Natural Clay

DIXIE L. SHEAR, HAROLD W. OLSEN, AND KARL R. NELSON

Undisturbed and reconstituted specimens of a soft gray Pleistocene clay were subjected to various degrees of desiccation, resaturated, and then tested to determine their hydraulic conductivity ($k$) versus void ratio ($e$) relationships. The log $k$ versus $e$ relationships for all of the specimens have a common shape that is characterized by a steep slope at high void ratios and a much flatter slope at lower void ratios. Desiccation affected primarily the magnitude, and not the shape, of the log $k$ versus $e$ relationships. With increasing degrees of desiccation, the relationships were displaced in the direction of increasing hydraulic conductivity. The desiccation-induced changes for the undisturbed specimens were greater than those exhibited by the reconstituted specimens. These characteristics of the log $k$ versus $e$ relationships can be explained in terms of the cluster model of clay fabric. At high void ratios, the steep slope of the log $k$ versus $e$ relationship is dominated by reductions in the sizes of the macropores surrounding the clusters. At lower void ratios, the increasing relative importance of pore-size reductions within the clusters is reflected in the decreasing slope of the log $k$ versus $e$ relationship. The generally higher hydraulic conductivity values with increasing degrees of desiccation in both the undisturbed and reconstituted samples reflect desiccation-induced shrinkage of clusters.

The macroscopic effects of desiccation on fine-grained soils are well known. In nature, near-surface materials are often overconsolidated, and very fine-grained clays such as smectite develop large cracks and fissures in response to desiccation.

The microscopic responses of soil fabric to desiccation are less well known due to the limitations of existing methods for observing these effects. Existing data show that remolded materials undergo greater shrinkage than undisturbed materials during desiccation because the pore sizes are smaller in the remolded materials (*1*). Pore-size distribution studies using mercury intrusion porosimetry show that oven drying has large effects on both the size of macropores surrounding soil aggregates and the size of micropores within aggregates (*2,3*).

The question arises whether air drying significantly affects the fabric of fine-grained materials. This paper presents new evidence concerning the effects of desiccation induced by air drying on the hydraulic conductivity ($k$) versus void ratio ($e$) relationship for a natural clay and shows how these effects can be attributed to fabric changes induced by desiccation. These effects have the potential to damage the integrity of clay liners and covers used for liquid retention structures and waste containment facilities.

D. L. Shear, USPCI, 5665 Flatiron Parkway, Boulder, Colo. 80301. H. W. Olsen, Branch of Geologic Risk Assessment, U.S. Geological Survey, Box 25046, Mail Stop 966, Denver, Colo. 80225. K. R. Nelson, Department of Engineering, Colorado School of Mines, Golden, Colo. 80401.

## EXPERIMENTS

### Material Properties and Specimen Preparation

The natural clay used in this investigation was obtained with a Shelby tube sampler from a depth of 15 to 17 ft in the Talbot Formation at Carroll Island, Maryland. This formation is a Pleistocene coastal plain deposit of variable thickness that overlies pre-Cambrian rocks and Cretaceous formations (*4*). The material is a soft gray, slightly organic, and well-graded silty clay. It has a liquid limit of 34.8 percent, a plastic limit of 24.0 percent, a plasticity index of 10.8 percent, a clay-size fraction of 22 percent, a specific gravity of 2.73, and a natural void ratio of 0.86.

Undisturbed specimens were trimmed from the main sample to a diameter of 2½ in. and height of approximately ½ in. A stainless steel cutter and a Teflon-lined stainless steel ring, which served as the fixed ring apparatus during consolidation testing, were used. The initial sample height, diameter, and water content (indicated by the trimmings) were recorded. Each specimen was placed on a porous stone in a ceramic dish and sealed with plastic film. A small puncture was made in the center of the plastic, through which slow, uniform desiccation of the clay specimen was assumed to have occurred. The clay was permitted to air dry to a preselected water content. Sample height, diameter, and water content were again recorded to reflect the desiccation-induced changes in soil phase relationships.

The reconstituted specimens were prepared from air-dried trimmings of the main sample. These trimmings were broken down to a grain size passing through a #40 standard sieve, rewetted with distilled water, and mixed to form a viscous slurry. The slurry was placed under a vacuum to aid in saturation and eliminate air voids, and then carefully poured into a Teflon-lined stainless steel ring. Upper and lower porous stones and filter paper were used to confine the slurry solids but allow excess pore water to drain freely. The slurry was uniaxially compressed at a constant rate to a precalculated height and water content that reflected an initial void ratio similar to that of the undisturbed specimens. When this initial, reconstituted state was achieved, each sample was trimmed and permitted to desiccate in the same manner described for the undisturbed materials.

TABLE 1 Water Contents and Void Ratios of the Test Specimens

| Test Specimens | Before Desiccation | | After Desiccation | | Change |
|---|---|---|---|---|---|
| | (w%) | (e) | (w%) | (e) | (Δw%) |
| Undisturbed | | | | | |
| U-1 | 31 | 0.95 | 31 | 0.95 | 0 |
| U-2 | 30 | 0.84 | 25 | 0.78 | 5 |
| U-3 | 29 | 0.85 | 11 | 0.79 | 18 |
| U-4 | 30 | 0.84 | 7 | 0.77 | 23 |
| Reconstituted | | | | | |
| R-1 | 34 | 0.87 | 34 | 0.87 | 0 |
| R-2 | 30 | 0.81 | 21 | 0.70 | 9 |
| R-3 | 31 | 0.83 | 18 | 0.68 | 13 |
| R-4 | 30 | 0.88 | 9 | 0.74 | 21 |
| R-5 | 32 | 0.86 | 6 | 0.71 | 26 |

Four undisturbed and five reconstituted specimens were prepared and air dried to varying degrees of desiccation. Table 1 gives, for each of the specimens, the water content ($w$) and void ratio ($e$) before and after desiccation, and the change in water content ($\Delta w$) during desiccation.

## Experimental System and Procedures

The specimens were tested in a recently developed (*5,6*) volume-controlled apparatus for simultaneous direct measurement of one-dimensional consolidation and hydraulic conductivity, shown in Figure 1. This apparatus consists of an Anteus (use of trade names in this report is for descriptive purposes only and does not imply endorsement by the U.S. Geological Survey) one-dimensional backpressure oedometer equipped with two flow pumps. One pump (F) transmits fluid to the load pressure chamber (L) and thereby provides a means to consolidate a test specimen (S) at a constant rate of volume change, which is commonly referred to as a constant-rate-of-deformation (CRD) test. The second flow pump (P) controls pore-fluid movement across the base of the specimen and thereby provides a means to conduct constant-flow hydraulic conductivity tests simultaneously with a CRD consolidation test.

Figure 2 shows a typical time history for a test, taken from an actual analog strip chart recording. The variations in effective stress, base pore pressure, and void ratio are plotted separately. The specimen was first equilibrated under a small and constant seating load for more than 12 hr. The void ratio initially decreased slightly and then remained almost constant. Hydraulic conductivity was measured periodically by withdrawing pore fluid from the base of the specimen at a constant rate and monitoring the induced pore-pressure changes at the base of the specimen. Following this initial period, the specimen was consolidated at a constant rate of deformation until the total elapsed time reached about 65 hr. The upper graph shows the buildup of vertical effective stress with time, and the middle graph shows the consolidation-induced pore pressure at the base of the specimen, designated as the "compression baseline." Superimposed hydraulic conductivity tests are reflected in periodic changes in base pore pressure from the compression baseline that were induced by withdrawing pore fluid from the base of the sample at a constant rate. When compression was terminated, the base pore pressure returned to zero, and the vertical effective stress decayed somewhat, apparently because of some combination of secondary compression and equipment compliance. During rebound, the effective stress decreased with time (Figure 2 upper), and the rebound-induced change in base pore pressure, designated as the rebound baseline in Figure 2 (middle), was negative. The changes in base pore pressure induced by superimposed constant-flow hydraulic conductivity tests were clearly evident.

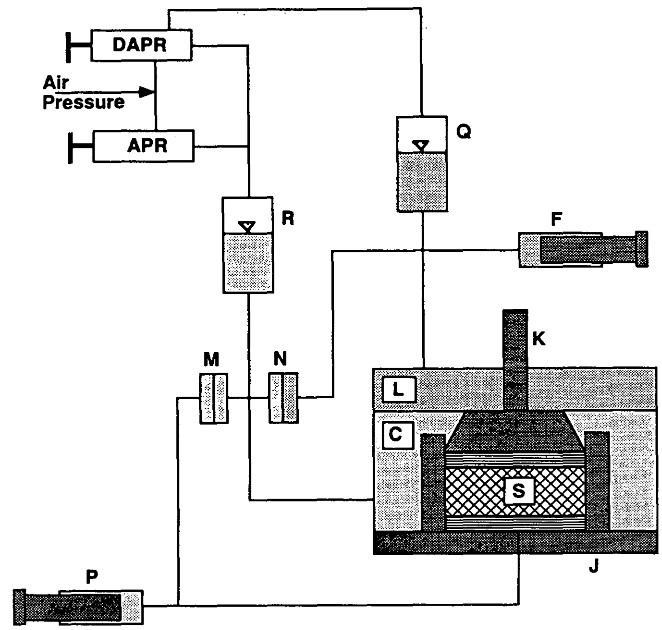


**FIGURE 1 Diagram of a backpressured consolidometer (J) equipped for constant-flow hydraulic conductivity measurements on a volume-controlled specimen (S). One flow pump (F) controls the specimen volume by infusing or withdrawing fluid into the hydraulic loading chamber (L). The thickness of the sample is monitored by a linear variable differential transducer (K), and the effective stress is monitored by a differential pressure transducer (N) in terms of the pressure difference between the loading chamber (L) and the backpressure chamber (C). A second flow pump (P) infuses or withdraws fluid across one end of the specimen (S) while flow across the opposite end moves to or from a pressure-controlled reservoir (R). The differential pressure transducer (M) monitors the pressure difference across the specimen. APR and DAPR are air pressure and differential air pressure regulators, respectively. DAPR and the backpressure chamber (Q) provide a means of applying an initial seating load on the specimen.**

## RESULTS

The measured log $k$ versus $e$ relationships for the undisturbed and reconstituted specimens are presented in Figures 3 and 4, respectively. In both figures, each specimen is designated by its water content after desiccation. Increasing degrees of desiccation are characterized by decreasing water content values, compared with the initial water contents of the specimens before desiccation, which were shown in Table 1 to be on the order of 30 percent. Also shown in each figure is a line labeled "K C Equation." These lines show the variation of hydraulic conductivity with void ratio predicted by the Kozeny-Carman equation assuming all factors have arbitrary constant values

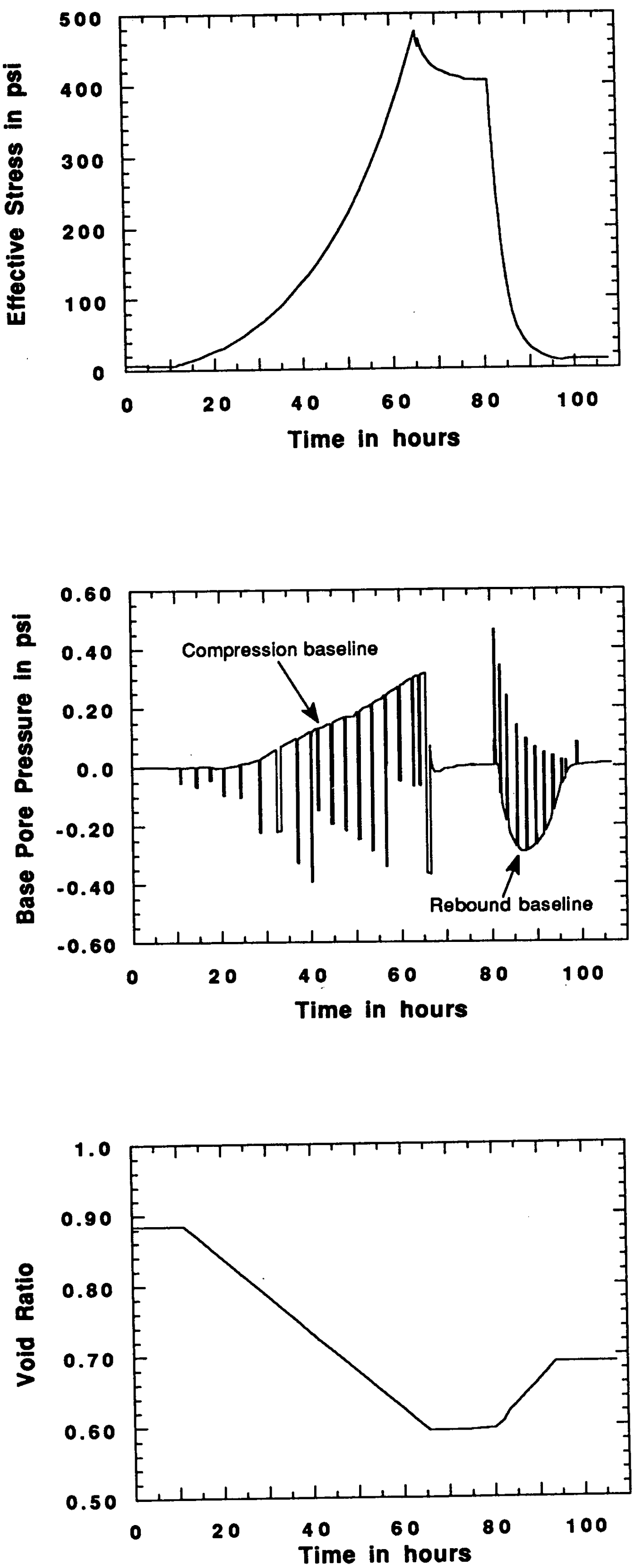


FIGURE 2 Time history of simultaneous constant-flow hydraulic conductivity and continuous-loading compressibility measurements in the one-dimensional consolidometer shown in Figure 1.

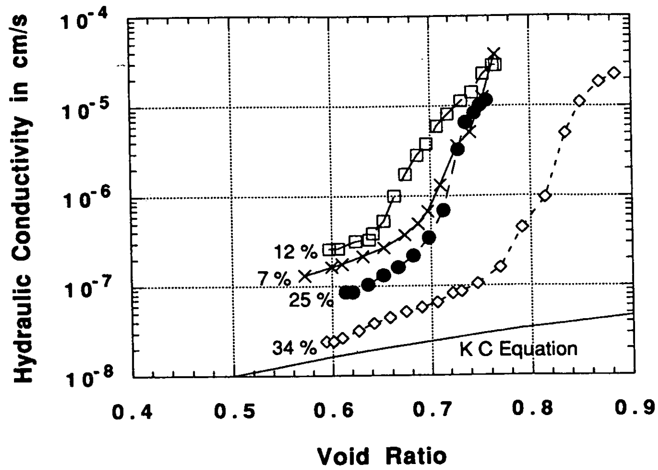


FIGURE 3 Log $k$ versus $e$ relationships for undisturbed specimens. The curve for each specimen is designated by the water content of the specimen after desiccation.

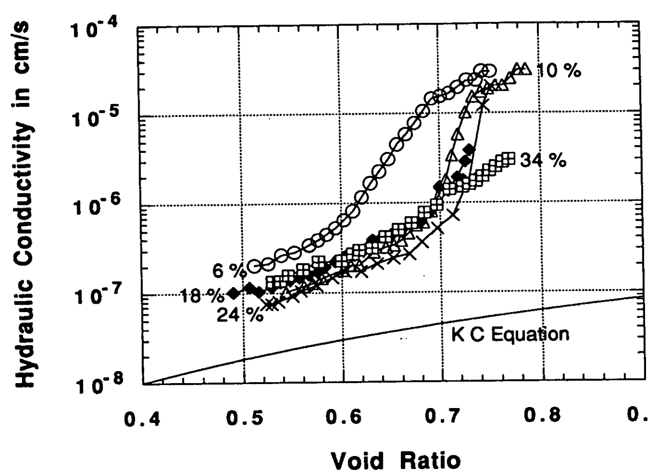


FIGURE 4 Log $k$ versus $e$ relationships for reconstituted specimens. The curve for each specimen is designated by the water content of the specimen after desiccation.

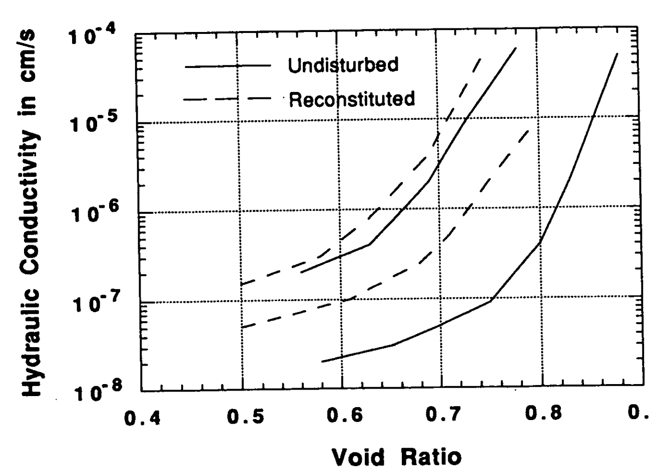


FIGURE 5 Comparison of ranges between upper and lower bounds of log $k$ versus $e$ relationships for the undisturbed and reconstituted specimens.

except void ratio. This equation is

$$k = \left(\frac{\gamma}{\mu}\right)\left(\frac{1}{k_o T^2 S_o^2}\right)\left(\frac{e}{1 + e}\right) \tag{1}$$

where

$k$ = hydraulic conductivity,
$\mu$ = viscosity,
$\gamma$ = density of the pore fluid,
$k_o$ = shape factor,
$T$ = tortuosity of the pore space,
$S_o$ = specific surface area per unit volume of particles, and
$e$ = void ratio.

All of the log $k$ versus $e$ relationships have a common shape that is characterized by a steep slope at high void ratios and a much flatter slope at lower void ratios. The pronounced change in slope of these relationships and the discrepancies between these slopes and that predicted by the Kozeny-Carman equation are well-known characteristics that have been observed in numerous previous studies, as discussed later in this paper.

The influence of desiccation appears to be twofold. First, the position of the log $k$ versus $e$ plots for individual specimens changes; however, the overall shape of each plot remains the same. Second, the general trend of the individual curve shift is toward increasing magnitudes of hydraulic conductivity, in accordance with increasing desiccation state in each specimen suite. Exceptions to these trends involve one undisturbed specimen designated with a water content of 7 percent and two reconstituted specimens designated with water contents of 9 and 34 percent.

Figure 5 compares the overall magnitudes of the desiccation effects on the undisturbed and reconstituted specimens. The width of the band between the upper and lower bounds for the undisturbed specimens is more than twice that for the reconstituted specimens. This difference in bandwidth reflects primarily a difference in the lower bounds of hydraulic conductivity values of the undesiccated specimens of both undisturbed and reconstituted materials. In contrast, there is little difference between the upper bounds of hydraulic conductivity values for the desiccated specimens of both undisturbed and reconstituted materials.

## DISCUSSION OF RESULTS

It has long been recognized that large discrepancies occur between measured and theoretical $k$ versus $e$ relationships in fine-grained soils (*7–10*). These discrepancies arise for theoretical relationships derived from capillary tube models of porous media that assume that the pores are uniform in size. The most widely known of these relationships is the Kozeny-Carman equation, which was introduced as Equation 1 and plotted in Figures 3 and 4.

Figure 6 shows these discrepancies with data published by Olsen (*10*) and reproduced by Mitchell (*1*). The discrepancies are expressed in terms of the ratio of the measured to predicted hydraulic conductivities; the latter were calculated from Equation 1. A horizontal line on this graph represents the

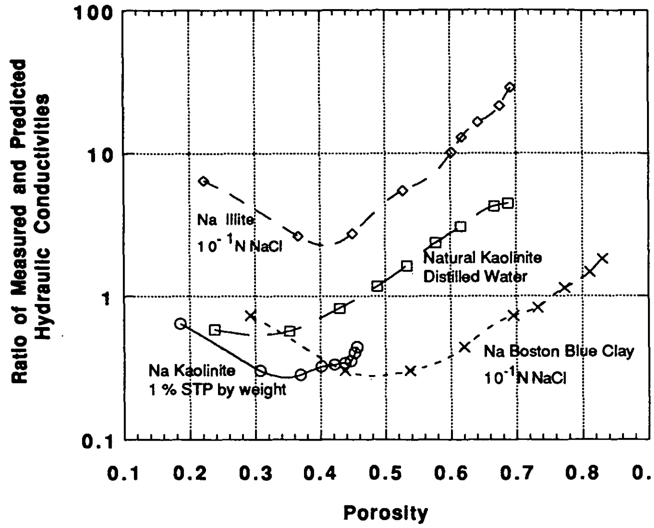


**FIGURE 6 Ratio of measured and predicted hydraulic conductivities (*10*).**

specific case in which the rate of change of hydraulic conductivity with porosity is the same for both measured and predicted values. During compression at high porosities (or void ratios), hydraulic conductivity decreases more rapidly with decreasing porosity than is predicted by Equation 1. Conversely, for compression at very low porosities, hydraulic conductivity decreases less rapidly than predicted by Equation 1. Note that the same behavior occurs for a variety of clays and pore fluids. The discrepancies in Figure 6 for porosities greater than about 0.4 ($e$ = 0.67) have the same characteristics as those in Figure 3 and 4. The data in Figure 6 for porosities less than about 0.4 ($e$ = 0.67) were obtained at much higher effective stresses than were used to obtain the data in Figures 3 and 4. Therefore, the characteristics of the discrepancies at low porosities in Figure 6 do not appear in Figures 3 and 4.

The fundamental cause of these discrepancies was identified as unequal pore sizes by Olsen in 1962 (*10*). Figure 7 shows the fabric model Olsen introduced to differentiate pore space into macropores surrounding clusters of particles and micropores within the clusters. Because fluid flow through soil pores is proportional to the fourth power of the pore radii, flow through the micropores is negligible compared with flow through the macropores.

Olsen's explanation for the discrepancies also required the assumption that during compression at high void ratios, the macropore sizes are reduced by rearrangement of the clusters, whereas the micropore sizes within the clusters are unaffected. At lower void ratios, after the clusters have been rearranged into a state of minimum packing, compression reduces both the macropore and micropore sizes. Figure 8 shows these changes in the macropore and micropore sizes as follows. The abscissa shows the total void ratio, $e_T$, and the ordinate shows the macropore and micropore components of the total void ratio in terms of the intercluster void ratio, $e_p$, and the cluster void ratio, $e_c$. With decreasing values of total void ratio, the cluster void ratio remains constant until its intercluster void ratio decreases to a value of 0.43, which is the void ratio for the densest possible packing of uniform-sized spheres. Below this critical void ratio, Figure 8 shows compression occurring

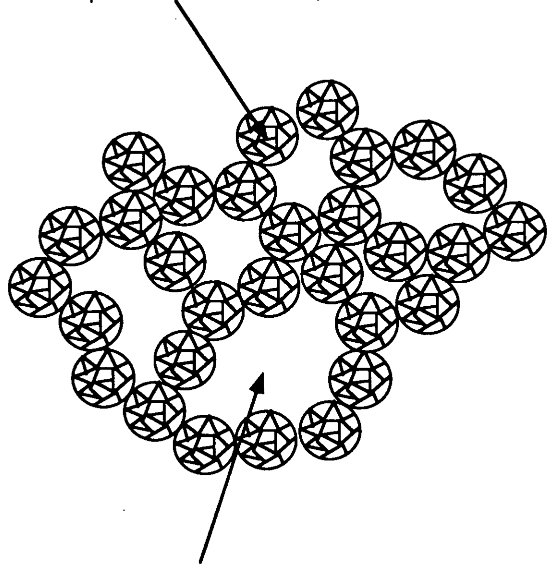


**FIGURE 7 Cluster model (*10*).**

During the last two decades, mercury intrusion porosimetry and electron microscopy studies have confirmed that the hydraulic conductivity of clays is governed by their pore-size distributions (*11*). These studies have also shown that clay pores are distributed among macropores surrounding assemblages of particles, minipores within aggregations of particle groups, and micropores between adjacent particles. Figure 9 is a recently published illustration (*12*) of the widely quoted fabric model derived from electron microscopy studies by Collins and McGown in 1974 (*13*). The particle assemblages in this model correspond to the clusters in Olsen's model. In Collins and McGown's model the macropores that govern hydraulic flow exist between particle assemblages. Much smaller pores exist within the assemblages, including micropores between individual particles and minipores between particle groups. In Olsen's model the macropores governing hydraulic flow existing between the clusters are designated as intercluster pores. The smaller micropores and minipores within the clusters are referred to as intracluster pores.

More recent electron microscopy and mercury intrusion porosimetry studies support the assumption in Figure 8 that the intracluster void ratio remains constant during compression at high void ratios. These studies show that the volume decrease during consolidation of soft clays is due to changes in the volume of the largest existing pores; only minor to negligible changes in the micropores have been observed (*3,12,14–16*).

both within and between the clusters. In relation to Figures 3, 4, and 6, the very rapid decrease in log *k* versus *e* at the highest void ratios corresponds with compression involving only the macropores between clusters. At lower void ratios, the less rapid decrease in log *k* versus *e* reflects a decreasing rate of volume change in the macropores because part of the volume change involves compression of the clusters.

Desiccation influences the position of the log *k* versus *e* relationships in Figure 3 to 5. It is recognized that the capillary forces induced by desiccation increase in magnitude with decreasing pore size. In the cluster model, desiccation causes shrinkage of the clusters, and increasing degrees of desiccation

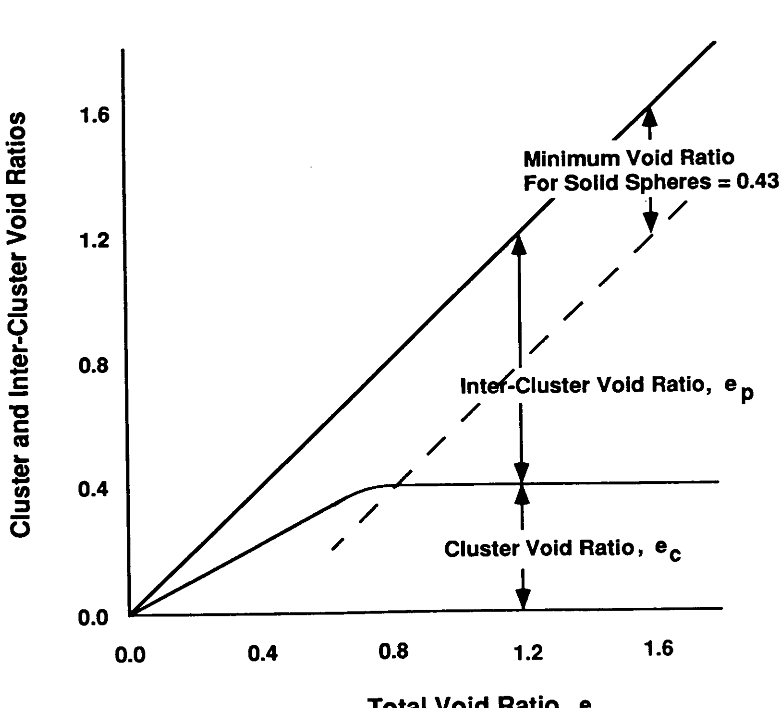


**FIGURE 8 Assumed relationships between total ($e_T$), cluster ($e_c$), and intercluster ($e_p$) void ratios for two specimens having different initial cluster void ratios when consolidated from a slurry (*10*).**

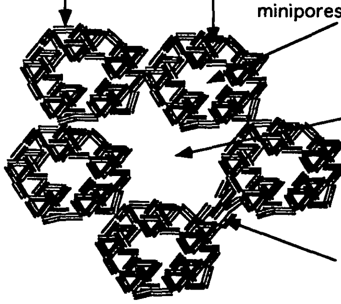


**FIGURE 9 Fabric elements and pore types, interpreted from Collins and McGown (*13*) by Griffiths and Joshi (*12*).**

cause decreasing magnitudes of cluster void ratios. When the log *k* versus *e* curves in either Figure 3 or Figure 4 are compared at the same total void ratio, the more desiccated specimens have smaller cluster void ratios and larger intercluster void ratios. Therefore, the more desiccated specimens have larger macropores and higher hydraulic conductivities. This trend is clearly evident in Figure 3 and appears to a lesser extent in Figure 4. In Figure 5, the range in values, or bandwidth, is small for the reconstituted specimens. Because the specimens were prepared from air-dried materials, the primary effects of desiccation took place before these specimens were tested. In contrast, the wide bandwidth for the undisturbed specimens reflects the full range of desiccation effects.

The data presented in Figures 3 and 4 include some inconsistencies with the trends described for the undisturbed specimen designated with a water content of 7 percent and for the reconstituted specimens designated with water contents of 9 and 34 percent. Whether these inconsistencies are due to variability of the materials in the test specimens or to fabric complexities not recognized in the cluster model has yet to be determined.

## CONCLUSIONS

Undisturbed and reconstituted specimens of a soft gray Pleistocene clay were subjected to various degrees of desiccation, resaturated, and then tested to determine their hydraulic conductivity (*k*) versus void ratio (*e*) relationships. The log *k* verus *e* relationships for all of the specimens exhibited pronounced curvature in the direction of decreasing rates of change in log *k* with decreasing void ratios. Desiccation affected primarily the magnitude, and not the shape, of the log *k* versus *e* relationships. With increasing degrees of desiccation, the relationships were displaced in the direction of increasing hydraulic conductivity. The desiccation-induced changes for the undisturbed specimens were greater than those exhibited by the reconstituted specimens.

These characteristics of the log *k* versus *e* relationships can be explained in terms of the cluster model of clay fabric. At high void ratios, the steep slope of the log *k* versus *e* relationship is dominated by reductions in the sizes of the macropores surrounding the clusters. At lower void ratios, the increasing relative importance of pore-size reductions within the clusters is reflected in the decreasing slope of the log *k* versus *e* relationship. The generally higher hydraulic conductivity values with increasing degrees of desiccation in both the undisturbed and reconstituted samples reflect desiccation-induced shrinkage of clusters. This process modifies the pore-size distribution by reducing the proportion of the void space in the micropores within clusters compared with the void space in the macropores between clusters. This mechanism also accounts for the generally higher hydraulic conductivity values in the reconstituted samples, because they were prepared from air-dried materials.

## REFERENCES

1. J. K. Mitchell. *Fundamentals of Soil Behavior.* John Wiley and Sons, New York, 1976, 450 pp.
2. S. Diamond. Pore Size Distribution in Clays. *Clays and Clay Minerals*, Vol. 18, 1970, pp. 7–23.
3. P. Delage and G. LeFebvre. Study of the Structure of a Sensitive Champlain Clay and Its Evolution During Consolidation. *Canadian Geotechnical Journal*, Vol. 21, 1984, pp. 21–35.
4. R. R. Bennett and R. R. Meyer. Geology and Ground-Water Resources of the Baltimore Area, In *Bulletin No. 4*, Department of Geology, Mines, and Water Resources, Board of Natural Resources, State of Maryland, 1952, pp. 24–72.
5. J. D. Gill. *Simultaneous Measurement of Compressibility and Hydraulic Conductivity Using Volume-Controlled Methods.* M.S. thesis. Colorado School of Mines, Golden, Colo. 1989, 184 pp.
6. J. D. Gill, H. W. Olsen, and K. R. Nelson. Volume-Controlled Approach for Direct Measurement of Compressibility and Hydraulic Conductivity. *Proc.*, *Geotechnical Engineering Congress 1991*, ASCE Geotechnical Special Publication 27, 1991, pp. 1100–1111.
7. C. Terzaghi. Principles of Soil Mechanics: III-Determination of Permeability of Clay. *Engineering News Record*, Vol. 95, 1925, pp. 832–836.
8. H. H. Macey. Clay-Water Relationships and the Internal Mechanism of Drying. *Transactions, British Ceramic Society*, Vol. 41, 1942, pp. 73–121.
9. A. S. Michaels and C. S. Lin. The Permeability of Kaolinite. *Industrial and Engineering Chemistry*, Vol. 46, 1954, pp. 1239–1246.
10. H. W. Olsen. Hydraulic Flow Through Saturated Clays. *Proc.*, *Ninth National Conference on Clays and Clay Minerals*, 1962, pp. 131–161.
11. I. Garcia-Bengochea, C. W. Lovell, and A. G. Altshaeffl. Pore Distribution and Permeability of Silty Clays. *Journal of the Geotechnical Engineering Division*, American Society of Civil Engineers, Vol. 105, No. GT7, 1979, pp. 839–855.
12. F. J. Griffiths and R. C. Joshi. Clay Fabric Response to Consolidation. *Applied Clay Science*, Vol. 5, 1990, pp. 37–66.
13. K. Collins and A. McGown. The Form and Function of Microfabric Features in a Variety of Natural Soils. *Geotechnique*, Vol. 24, 1974, pp. 223–254.
14. P. Delage. Microstructure and Compressibility of Some Eastern Canadian Sensitive Soft Clays. *Proc.*, *International Symposium on Geotechnical Engineering of Soft Soils, Mexico*, Vol. 1, 1987, pp. 33–38.
15. F. J. Griffiths and R. C. Joshi. Change in Pore-Size Distribution due to Consolidation of Clays. *Geotechnique*, Vol. 39, 1989, pp. 159–167.
16. T. S. Nagaraj, A. Vatsala, and B. R. Srinivasa Murthy. Discussion of Change in Pore Size Distribution due to Consolidation of Clays, F. J. Griffiths and R. C. Joshi, *Geotechnique*, Vol. 40, No. 2, 1990, pp. 303–309.

*Publication of this paper sponsored by Committee on Soil and Rock Properties.*